RESEARCH ARTICLE | AUGUST 20 2026

Memory kernel non-additivity in the generalized quantum master equation for a system coupled to multiple heat baths

Callie Wilson ; Xiaohan Dan ; Victor S. Batista ; Eitan Geva

J. Chem. Phys. 165, 074117 (2026)
https://doi.org/10.1063/5.0346129

The Journal of Chemical Physics ARTICLE pubs.aip.org/aip/jcp

Memory kernel non-additivity in the generalized quantum master equation for a system coupled to multiple heat baths

Cite as: J. Chem. Phys. 165, 074117 (2026); doi: 10.1063/5.0346129
Submitted: 1 June 2026 • Accepted: 3 August 2026 •
Published Online: 20 August 2026

Callie Wilson,[1] Xiaohan Dan,[2] Victor S. Batista,[2] and Eitan Geva[1,a)]

AFFILIATIONS

[1] Department of Chemistry, University of Michigan, Ann Arbor, Michigan 48109, USA
[2] Department of Chemistry, Yale University, New Haven, Connecticut 06520, USA

[a)] Author to whom correspondence should be addressed: eitan@umich.edu

ABSTRACT

The generalized quantum master equation provides an exact equation of motion for the reduced density operator of a quantum system coupled to one or more baths, with all bath-induced effects encoded in a memory kernel superoperator. In this paper, we investigate whether the memory kernel for a system coupled simultaneously to multiple independent baths can be written as a sum of memory kernels associated with the corresponding single-bath problems. We show that such additivity holds in the weak system–bath coupling limit, where the second-order memory kernel separates into independent bath contributions. Beyond this limit, however, the baths become dynamically correlated through their mutual coupling to the system, and the exact multi-bath memory kernel is no longer equal to the sum of exact single-bath memory kernels. We demonstrate this non-additivity for a two-level system linearly coupled to hot and cold harmonic baths, using the hierarchical equations of motion method to construct the memory kernels. The results show that non-additivity increases with system–bath coupling strength and is process-dependent: coherence damping remains comparatively well described by an additive kernel, whereas population–coherence and coherence–coherence transfer exhibit pronounced non-additive behavior. These findings clarify the limitations of additive multi-bath descriptions and highlight the ambiguity of decomposing heat flow into independent bath-resolved contributions beyond weak system–bath coupling.

I. INTRODUCTION

Open quantum system dynamics is often modeled based on the assumption that the system is coupled to a single bath at thermal equilibrium with respect to a single well-defined temperature.[1–6] However, real systems often interact simultaneously with multiple baths composed of different subsets of degrees of freedom, each characterized by distinct thermodynamic conditions such as temperature or chemical potential, thereby driving the system out of equilibrium. Such situations arise, for example, in molecular junctions, quantum thermal transport setups, nanoscale heat engines, and driven condensed-phase systems.[7–23] The presence of multiple nonequilibrated environments raises a fundamental question: is the cumulative effect of the baths on the system dynamics equal to the sum of the effects that each bath would exert in isolation?

At the limit of weak system–bath coupling, the answer is yes. In particular, when the system–bath coupling terms are treated as small perturbations within the framework of second-order time-dependent perturbation theory, the bath-induced contribution to the reduced dynamics is expressed in terms of equilibrium bath correlation functions of the individual baths.[1–6] As a result, the second-order memory kernel separates into a sum of independent bath contributions, as discussed in Sec. II D. This additivity underlies standard weak-coupling quantum master equations, where relaxation rates can be written as sums of bath-resolved terms.

Beyond weak system–bath coupling, this additive structure no longer holds. Even when the baths are initially independent and there is no direct bath–bath interaction, the baths can become dynamically correlated through their mutual interaction with the system. Consequently, the effect of one bath on the system may

depend on whether the other bath is also present. Deviations from additivity, therefore, provide a direct probe of bath–bath correlations generated indirectly through the system, as discussed in Sec. II C.

Additivity of the bath-induced impact on the system, or lack thereof, is also closely connected to the definition of heat flows between the system and the baths, which is important for understanding heat formation and distribution in quantum devices and molecular junctions.[7–18,23,24] In classical thermodynamics,[25] the heat flow between a system and multiple baths is assumed to be additive. For example, in the case of a system coupled to two heat baths, hot and cold, the rate of change of the system energy is assumed to be given by

$$\dot{U} = \dot{Q}_h + \dot{Q}_c, \tag{1}$$

where U is the system energy, $\dot{Q}_h$ is the heat flux associated with the hot bath, and $\dot{Q}_c$ is the heat flux associated with the cold bath. In such an additive description, $\dot{Q}_h$ is assumed to be the same as it would have been in the absence of the cold bath, and $\dot{Q}_c$ is assumed to be the same as it would have been in the absence of the hot bath. This decomposition is natural for macroscopic systems, where the interaction between the system and each bath occurs at the interface at the point of contact and is, therefore, weak compared with the bulk energies. For microscopic quantum systems strongly coupled to baths, however, the system–bath interaction energy can become comparable to the system energy, and a unique bath-resolved decomposition of heat flow is no longer obvious.[26]

In this paper, we examine the additivity of bath-induced effects from the point of view of the generalized quantum master equation (GQME). The GQME provides an *exact* equation of motion for the reduced density operator of a quantum system coupled to one or more baths.[5,10,27–53] It is inherently non-Markovian and non-unitary and can accommodate multiple baths that may or may not be in thermal equilibrium relative to the other baths.

Within the GQME, all bath-induced effects are encoded in a memory kernel superoperator, $\mathcal{K}(t)$. Thus, for a system coupled to multiple baths, the question of additivity becomes the question of whether the exact multi-bath memory kernel can be decomposed into a sum of exact single-bath memory kernels. For example, in the case of a system coupled to two baths, hot and cold, this question can be written as

$$\mathcal{K}(t) \stackrel{?}{=} \mathcal{K}_h(t) + \mathcal{K}_c(t), \tag{2}$$

where $\mathcal{K}(t)$ is the exact memory kernel for the system coupled simultaneously to both baths, while $\mathcal{K}_h(t)$ and $\mathcal{K}_c(t)$ are the exact memory kernels for the corresponding hot (h) and cold (c) single-bath problems, respectively. This comparison is stronger than simply testing the validity of the weak-coupling approximation: it asks whether the exact influence of two independent baths is equivalent to the sum of two exact one-bath influences.

We show that Eq. (2) holds in the weak system–bath coupling limit but fails at stronger coupling. The non-additive component,

$$\Delta\mathcal{K}(t) = \mathcal{K}(t) - \mathcal{K}_h(t) - \mathcal{K}_c(t), \tag{3}$$

therefore quantifies the collective effect of coupling the system to both baths simultaneously. Importantly, this non-additivity is not uniform across the memory kernel. Different matrix elements of $\mathcal{K}(t)$ describe different bath-induced dynamical processes, including phase damping, population-to-coherence transfer, coherence-to-population transfer, and coherence-to-coherence transfer. As a result, the degree of non-additivity can depend on the specific process through which the baths affect the system dynamics.

We demonstrate these ideas for a two-level system linearly coupled to two harmonic baths held at different temperatures. The model is simple enough to allow a transparent analysis but rich enough to exhibit non-Markovian dynamics, strong system–bath coupling effects, and nonequilibrium heat transport. The quantum-mechanically exact memory kernels are calculated via the hierarchical equations of motion (HEOM) method,[54–57] which allows us to compare the exact two-bath memory kernel directly with the sum of the exact one-bath memory kernels.

The results reveal three main trends. First, the GQME with the exact multi-bath memory kernel reproduces the exact HEOM dynamics, while the additive approximation $\mathcal{K}_h(t) + \mathcal{K}_c(t)$ becomes increasingly inaccurate as the system–bath coupling strength increases. Second, the breakdown of additivity is process dependent: the phase-damping-related kernel element remains comparatively well described by an additive form, whereas population–coherence and coherence–coherence transfer show pronounced non-additive behavior. Third, the non-additivity of the memory kernel sheds new light on why decomposing the system-energy change into independent bath-resolved heat currents becomes ambiguous beyond weak coupling. Bath-resolved currents can still be introduced by specifying how the system–bath interaction energy is assigned. As a result, such current decompositions are convention dependent and cannot be uniquely inferred from the exact reduced system dynamics alone.[9]

The remainder of this paper is organized as follows. The GQME formalism for a system coupled to multiple baths is outlined and discussed in Sec. II, with emphasis on the additivity of the memory kernel, or lack thereof. A demonstrative application to a model of a two-level system linearly coupled to hot and cold harmonic baths is provided in Sec. III. Finally, concluding remarks are presented in Sec. IV. Technical details on the HEOM method used for calculating the memory kernels are provided in the Appendix.

II. THEORY

In this section, we outline the theoretical framework for the GQME of a system coupled to multiple baths. To this end, we follow the convention that a hat over a symbol, e.g., $\hat{A}$, indicates that the quantity is an operator, and a calligraphic font, e.g., $\mathcal{L}$, indicates that the quantity is a superoperator (i.e., an operator in Liouville space[58]).

A. Preliminary considerations

We consider a system coupled to multiple baths, described by the following Hamiltonian:

$$\hat{H} = \hat{H}_s + \hat{H}_b + \hat{H}_{bs}, \tag{4}$$

where $\hat{H}_s$ is the system Hamiltonian, $\hat{H}_b$ is the multiple baths Hamiltonian, and $\hat{H}_{bs}$ represents the interaction between the system and the baths.

For the sake of simplicity, we focus on the case of two heat baths at different temperatures (hot and cold), noting that all conclusions can be straightforwardly generalized to an arbitrary number of baths,

$$\hat{H}_b = \hat{H}_h + \hat{H}_c. \tag{5}$$

Here, $\hat{H}_h$ is the hot bath Hamiltonian and $\hat{H}_c$ is the cold bath Hamiltonian (each defined as a Hermitian operator in its own Hilbert space). The system–bath interactions can, without loss of generality, be expressed as a sum of tensor products of system and bath operators,

$$\hat{H}_{bs} = \hat{H}_{sh} + \hat{H}_{sc} = \sum_j \hat{B}_{hj} \otimes \hat{S}_j + \sum_j \hat{B}_{cj} \otimes \hat{S}_j. \tag{6}$$

Here, $\{\hat{S}_j\}$ are the system operators, $\{\hat{B}_{hj}\}$ are the hot bath operators, and $\{\hat{B}_{cj}\}$ are the cold bath operators (the explicit forms of these operators are system-specific and will be specified in Sec. III for the demonstrative model under consideration).

In what follows, we will also assume, without loss of generality, that

$$\mathrm{Tr}_h\left(\hat{\rho}_h^{eq}\hat{H}_{sh}\right) = \mathrm{Tr}_c\left(\hat{\rho}_c^{eq}\hat{H}_{sc}\right) = 0. \tag{7}$$

Here, Tr_h is the partial trace over the hot bath Hilbert space, Tr_c is the partial trace over the cold bath Hilbert space, and $\hat{\rho}_h^{eq}$ and $\hat{\rho}_c^{eq}$ are the density operators that correspond to the hot and cold baths being in thermal equilibrium,

$$\hat{\rho}_h^{eq} = \frac{e^{-\beta_h \hat{H}_h}}{Z_h}, \qquad \hat{\rho}_c^{eq} = \frac{e^{-\beta_c \hat{H}_c}}{Z_c}, \tag{8}$$

where $\beta_h = 1/k_B T_h$ is the inverse temperature of the hot bath (k_B is the Boltzmann's constant), $\beta_c = 1/k_B T_c$ is the inverse temperature of the cold bath, $Z_h = \mathrm{Tr}_h(e^{-\beta_h \hat{H}_h})$ is the partition function of the hot bath, and $Z_c = \mathrm{Tr}_c(e^{-\beta_c \hat{H}_c})$ is the partition function of the cold bath. The reason why Eq. (7) is valid without loss of generality is that one can always make it valid by redefining the system–bath coupling and system Hamiltonians such that

$$\begin{aligned} \hat{H}_{sh} &\to \hat{H}_{sh} - \mathrm{Tr}_h\left(\hat{\rho}_h^{eq}\hat{H}_{sh}\right), \\ \hat{H}_{sc} &\to \hat{H}_{sc} - \mathrm{Tr}_c\left(\hat{\rho}_c^{eq}\hat{H}_{sc}\right), \\ \hat{H}_s &\to \hat{H}_s + \mathrm{Tr}_h\left(\hat{\rho}_h^{eq}\hat{H}_{sh}\right) + \mathrm{Tr}_c\left(\hat{\rho}_c^{eq}\hat{H}_{sc}\right). \end{aligned} \tag{9}$$

Finally, we assume that the initial state of the overall system is given by a density operator of the following form:

$$\hat{\rho}(0) = \hat{\rho}_h^{eq} \otimes \hat{\rho}_c^{eq} \otimes \hat{\sigma}(0). \tag{10}$$

Here, $\hat{\rho}_h^{eq}$ and $\hat{\rho}_c^{eq}$ are defined as in Eq. (8), and $\hat{\sigma}(0)$ is the reduced density operator that describes the initial state of the system. Note that the system and baths are assumed to start out unentangled, with the baths in thermal equilibrium at their respective temperatures. Even though this is a commonly used form of the initial state, other choices are possible. Importantly, our approach is not limited to this form and can be straightforwardly extended to other choices of initial state, including ones where the baths are initially in nonequilibrium states and entangled with the system.

It should be noted that the multiple-bath Hamiltonian in Eq. (4) can alternatively be viewed as a *system coupled to a single composite bath*. However, this composite bath possesses a specific structure: (1) it consists of two distinct sub-baths that are not in mutual thermal equilibrium, although each sub-bath is individually thermalized at its own temperature. (2) The system–bath interaction is given by a sum of couplings to the individual sub-baths and does not include terms of the form $\hat{S} \otimes \hat{B}_h \otimes \hat{B}_c$, which could directly couple the sub-baths.

B. The generalized quantum master equation (GQME)

Next, we outline the formalism underlying the GQME, with emphasis on its application to a system with the Hamiltonian of the form of Eq. (4). Since the overall system is closed, the dynamics of the overall system density operator $\hat{\rho}(t)$ is governed by the following quantum Liouville equation:

$$\frac{d}{dt}\hat{\rho}(t) = -\frac{i}{\hbar}[\hat{H}, \hat{\rho}(t)] \equiv -\frac{i}{\hbar}\mathcal{L}\hat{\rho}(t). \tag{11}$$

In the next step, we define a projection superoperator $\mathcal{P}$ (an operator in the overall system's Liouville space), which satisfies $\mathcal{P}^2 = \mathcal{P}$. The equation of motion for the projection of $\hat{\rho}(t)$, $\mathcal{P}\hat{\rho}(t)$, is then given by the following *Nakajima–Zwanzig equation*:[27,28]

$$\begin{aligned} \frac{d}{dt}\mathcal{P}\hat{\rho}(t) = &-\frac{i}{\hbar}\mathcal{P}\mathcal{L}\mathcal{P}\hat{\rho}(t) - \frac{1}{\hbar^2}\int_0^t d\tau \mathcal{P}\mathcal{L}e^{-i\mathcal{Q}\mathcal{L}\tau/\hbar}\mathcal{Q}\mathcal{L}\mathcal{P}\hat{\rho}(t-\tau) \\ &- \frac{i}{\hbar}\mathcal{P}\mathcal{L}e^{-i\mathcal{Q}\mathcal{L}t/\hbar}\mathcal{Q}\hat{\rho}(0), \end{aligned} \tag{12}$$

where $\mathcal{Q}$ is the complementary projection operator defined by

$$\mathcal{Q} = \mathcal{I} - \mathcal{P}, \tag{13}$$

where $\mathcal{I}$ is the unity superoperator in the overall system Liouville space.

The specific choice of projection operator $\mathcal{P}$ is dictated by the choice of *dynamical quantity of interest*. In what follows, we will focus on a commonly used choice of dynamical quantity of interest, which corresponds to the reduced density operator that describes the state of the system at time t,

$$\hat{\sigma}(t) = \mathrm{Tr}_b[\hat{\rho}(t)]. \tag{14}$$

Here, $\mathrm{Tr}_b = \mathrm{Tr}_h\,\mathrm{Tr}_c$ (the partial trace over the Hilbert spaces of both baths) and $\hat{\rho}(t) = e^{-i\hat{H}t/\hbar}\hat{\rho}(0)e^{i\hat{H}t/\hbar} = e^{-i\mathcal{L}t/\hbar}\hat{\rho}(0)$.

Obtaining the equation of motion for $\hat{\sigma}(t)$ from Eq. (12) is facilitated by the following choice of projection operator:

$$\mathcal{P}\hat{A} = \hat{\rho}_h^{eq} \otimes \hat{\rho}_c^{eq} \otimes \mathrm{Tr}_b(\hat{A}). \tag{15}$$

Here, $\hat{\rho}_h^{eq}$ and $\hat{\rho}_c^{eq}$ are as in Eq. (8), and $\hat{A}$ is an overall system operator. Substituting $\mathcal{P}$ from Eq. (15) into Eq. (12) and partially tracing over the Hilbert spaces of both baths, we obtain[5]

$$\frac{d}{dt}\hat{\sigma}(t) = -\frac{i}{\hbar}\mathcal{L}_s\hat{\sigma}(t) - \int_0^t d\tau \mathcal{K}(\tau)\hat{\sigma}(t-\tau). \tag{16}$$

Here, $\mathcal{L}_s\hat{\sigma}(t) \equiv [\hat{H}_s, \hat{\sigma}(t)]$ and $\mathcal{K}(\tau)$ is the memory kernel superoperator, which is explicitly given by

$$\mathcal{K}(\tau) = \frac{1}{\hbar^2}\mathrm{Tr}_b\left\{\mathcal{L}e^{-i\mathcal{Q}\mathcal{L}\tau/\hbar}\mathcal{Q}\mathcal{L}\hat{\rho}_h^{eq}\otimes\hat{\rho}_c^{eq}\right\}. \tag{17}$$

It should be noted that Eq. (16) is the *quantum-mechanically exact equation of motion for* $\hat{\sigma}(t)$. In what follows, we will refer to Eq. (16) as the *GQME*. Importantly, other types of commonly used quantum master equations, such as the Lindblad[2] and Redfield quantum master equations,[1] correspond to approximate versions of the GQME, which are based on assuming weak system–bath coupling and Markovity and making the secular approximation (see Sec. II D).

Inspection of the GQME, Eq. (16), reveals that when $\mathcal{K}(\tau) \to 0$, the system can be treated as a *closed system*, whose dynamics is unitary and fully dictated by $\hat{H}_s$ via the quantum Liouville equation $d\hat{\sigma}(t)/dt = -i\mathcal{L}_s\hat{\sigma}(t)/\hbar$. Thus, $\mathcal{K}(\tau)$ fully captures the effect of the baths on the system's dynamics. The evaluation and analysis of $\mathcal{K}(\tau)$, therefore, offers a useful pathway for understanding the effect of the baths on the system's dynamics, which turns it from a unitary closed system dynamics into a non-unitary open system dynamics.

The memory kernel, $\mathcal{K}(\tau)$, can be calculated from so-called *projection free inputs (PFIs)*, i.e., inputs that do not explicitly feature $\mathcal{P}$ or $\mathcal{Q}$, via a variety of pathways.[47] In what follows, we will focus on one such pathway, where the system's time evolution superoperator, $\mathcal{U}(t)$, serves as the PFI. $\mathcal{U}(t)$ is defined as follows:

$$\hat{\sigma}(t) = \mathcal{U}(t)\hat{\sigma}(0) = \mathrm{Tr}_b\left(e^{-i\mathcal{L}t/\hbar}\hat{\rho}_h^{eq}\otimes\hat{\rho}_c^{eq}\otimes\hat{\sigma}(0)\right). \tag{18}$$

Given $\mathcal{U}(t)$, $\mathcal{K}(\tau)$ can be obtained by numerically solving the following integral Volterra equation:[42,44,59]

$$\mathcal{K}(\tau) = -\ddot{\mathcal{U}}(\tau) - \frac{i}{\hbar}\dot{\mathcal{U}}(\tau)\mathcal{L}_s - \int_0^\tau d\tau'\dot{\mathcal{U}}(\tau-\tau')\mathcal{K}(\tau'). \tag{19}$$

It should be noted that in practice, $\mathcal{U}(t)$ and $\mathcal{K}(\tau)$ are represented by $n^2 \times n^2$ matrices in terms of a basis of the system's Hilbert space of one's choice, where n is the dimension of the system's Hilbert space. More specifically, Eqs. (16) and (19) in matrix form are given by

$$\frac{d}{dt}\sigma_{jk}(t) = -\frac{i}{\hbar}\sum_{mn}\mathcal{L}_{s,jk,mn}\sigma_{mn}(t) - \sum_{mn}\int_0^t d\tau\mathcal{K}_{jk,mn}(\tau)\sigma_{mn}(t-\tau), \tag{20}$$

$$\mathcal{K}_{jk,mn}(\tau) = -\ddot{\mathcal{U}}_{jk,mn}(\tau) - \frac{i}{\hbar}\sum_{pq}\dot{\mathcal{U}}_{jk,pq}(\tau)\mathcal{L}_{s,pq,mn} - \sum_{pq}\int_0^\tau d\tau'\dot{\mathcal{U}}_{jk,pq}(\tau-\tau')\mathcal{K}_{pq,mn}(\tau'), \tag{21}$$

with $\sigma_{jk}(t) = \langle j|\hat{\sigma}(t)|k\rangle$ and the (jk,lm) matrix element of a system superoperator $\mathcal{A}(\tau)$ given by

$$\mathcal{A}_{jk,lm}(\tau) = \mathrm{Tr}\left\{|j\rangle\langle k|^\dagger\mathcal{A}(\tau)|l\rangle\langle m|\right\}, \tag{22}$$

where $\mathrm{Tr} = \mathrm{Tr}_s\,\mathrm{Tr}_h\,\mathrm{Tr}_c$ is the trace over the overall system's Hilbert space, $\mathcal{A} = \mathcal{L}_s, \mathcal{K}(\tau), \mathcal{U}(\tau), \dot{\mathcal{U}}(\tau)$, and $j,k,m,l,n,p,q = 1,\ldots,n$.

Finally, we note that the GQME approach is closely related to the transfer tensor method (TTM) of Cerrillo and Cao.[60] In particular, given the transfer tensor, one can extract a memory kernel that corresponds to a discretized version of the continuous-time memory kernel of the GQME approach[53] (although consistency between the two approaches appears to be sensitive to the discretization procedure[52]).

C. The non-additivity of the effect of the individual baths on the system's dynamics

The GQME in Eq. (16) is the exact equation of motion for a system coupled to *two* baths. Within Eq. (16), the memory kernel, $\mathcal{K}(\tau)$, as given by Eq. (17), fully captures the effect of the two baths on the system's dynamics. Generally speaking, the effect of the two baths on the system's dynamics is *non-additive*, i.e., it is not generally true that $\mathcal{K}(\tau)$ can be written as a sum of two memory kernels.

To see this, consider the case where the system is only coupled to the hot bath. The overall Hamiltonian for such a system is then given by

$$\hat{H}_\eta = \hat{H}_s + \hat{H}_h + \hat{H}_{sh}. \tag{23}$$

Following a similar procedure to that followed in Sec. II B, one can derive the following GQME for such a case:

$$\frac{d}{dt}\hat{\sigma}(t) = -\frac{i}{\hbar}\mathcal{L}_s\hat{\sigma}(t) - \int_0^t d\tau\mathcal{K}_h(\tau)\hat{\sigma}(t-\tau), \tag{24}$$

where

$$\mathcal{K}_h(\tau) = \frac{1}{\hbar^2}\mathrm{Tr}_h\left\{\mathcal{L}_{sh}e^{-i\mathcal{Q}_h\mathcal{L}_\eta\tau/\hbar}\mathcal{Q}_h\mathcal{L}_{sh}\hat{\rho}_h^{eq}\right\}. \tag{25}$$

Here, $\mathcal{L}_\eta\hat{A} = [\hat{H}_\eta, \hat{A}]$, $\mathcal{L}_{sh}\hat{A} = [\hat{H}_{sh}, \hat{A}]$, $\mathcal{P}_h\hat{A} = \hat{\rho}_h^{eq}\otimes\mathrm{Tr}_h(\hat{A})$, and $\mathcal{Q}_h = \mathcal{I} - \mathcal{P}_h$. Similarly, when the system is only coupled to the cold bath, the overall Hamiltonian is given by

$$\hat{H}_\kappa = \hat{H}_s + \hat{H}_c + \hat{H}_{sc}, \tag{26}$$

and the corresponding GQME is

$$\frac{d}{dt}\hat{\sigma}(t) = -\frac{i}{\hbar}\mathcal{L}_s\hat{\sigma}(t) - \int_0^t d\tau\mathcal{K}_c(\tau)\hat{\sigma}(t-\tau), \tag{27}$$

where

$$\mathcal{K}_c(\tau) = \frac{1}{\hbar^2}\mathrm{Tr}_c\left\{\mathcal{L}_{sc}e^{-i\mathcal{Q}_c\mathcal{L}_\kappa\tau/\hbar}\mathcal{Q}_c\mathcal{L}_{sc}\hat{\rho}_c^{eq}\right\}, \tag{28}$$

with $\mathcal{L}_\kappa\hat{A} = [\hat{H}_\kappa, \hat{A}]$, $\mathcal{L}_{sc}\hat{A} = [\hat{H}_{sc}, \hat{A}]$, $\mathcal{P}_c\hat{A} = \hat{\rho}_c^{eq}\otimes\mathrm{Tr}_c(\hat{A})$, and $\mathcal{Q}_c = \mathcal{I} - \mathcal{P}_c$. The non-additivity of $\mathcal{K}(\tau)$ then implies that

$$\mathcal{K}(\tau) \neq \mathcal{K}_h(\tau) + \mathcal{K}_c(\tau). \tag{29}$$

Importantly, the non-additivity of the memory kernel is a signature of strong system–bath coupling. As shown in Sec. II D, $\mathcal{K}(\tau)$ is additive, namely, $\mathcal{K}(\tau) = \mathcal{K}_h(\tau) + \mathcal{K}_c(\tau)$, in the limit of weak

system–bath coupling. Thus, $\mathcal{K}(\tau) - \mathcal{K}_h(\tau) - \mathcal{K}_c(\tau)$ can be used as a measure of the collective strong coupling effect, where the effect of being coupled to two baths is not the same as the sum of effects due to being coupled to the individual baths.

D. The limits of weak system–bath coupling, Markovian dynamics, and the secular approximation

Further insight into the aforementioned GQME for a system coupled to two baths can be obtained by considering its weak system–bath coupling limit. The weak system–bath coupling limit corresponds to truncating the expansion of the memory kernel, $\mathcal{K}(\tau)$, in powers of the system–bath coupling terms, $\hat{H}_{bs}$ [see Eq. (6)], at the lowest non-vanishing order, which corresponds to second order for the Hamiltonian under consideration.[5] Doing so for the memory kernel in Eq. (17) leads to the following weak-coupling approximation for the memory kernel:

$$\mathcal{K}(\tau) \approx \mathcal{K}^{(2)}(\tau) = \mathcal{K}_h^{(2)}(\tau) + \mathcal{K}_c^{(2)}(\tau), \tag{30}$$

where

$$\begin{aligned}\mathcal{K}_h^{(2)}(\tau) &= \frac{1}{\hbar^2}\mathrm{Tr}_h\left\{\mathcal{L}_{sh}e^{-i\mathcal{L}_h\tau/\hbar}e^{-i\mathcal{L}_s\tau/\hbar}\mathcal{L}_{sh}\hat{\rho}_h^{eq}\right\},\\ \mathcal{K}_c^{(2)}(\tau) &= \frac{1}{\hbar^2}\mathrm{Tr}_c\left\{\mathcal{L}_{sc}e^{-i\mathcal{L}_c\tau/\hbar}e^{-i\mathcal{L}_s\tau/\hbar}\mathcal{L}_{sc}\hat{\rho}_c^{eq}\right\}.\end{aligned} \tag{31}$$

Thus, the system dynamics in the limit of weak system–bath coupling is given by the following quantum master equation:

$$\frac{d}{dt}\hat{\sigma}(t) = -\frac{i}{\hbar}\mathcal{L}_s\hat{\sigma}(t) - \int_0^t d\tau\mathcal{K}_h^{(2)}(\tau)\hat{\sigma}(t-\tau) - \int_0^t d\tau\mathcal{K}_c^{(2)}(\tau)\hat{\sigma}(t-\tau). \tag{32}$$

Importantly, the effect of the two baths on the system dynamics is *additive* in the weak system–bath coupling limit. It consists of a sum of two terms, one which is solely due to the coupling to the hot bath, $-\int_0^t d\tau\mathcal{K}_h^{(2)}(\tau)\hat{\sigma}(t-\tau)$, and another, $-\int_0^t d\tau\mathcal{K}_c^{(2)}(\tau)\hat{\sigma}(t-\tau)$, which is solely due to the coupling to the cold bath.

Furthermore, $\mathcal{K}_h^{(2)}(\tau)$ and $\mathcal{K}_c^{(2)}(\tau)$ correspond to the weak coupling limit of $\mathcal{K}_h(\tau)$ and $\mathcal{K}_c(\tau)$ in Eqs. (25) and (28), respectively. This implies that the effect of the hot (cold) bath on the system is the same as it would have been if the system were only coupled to the hot (cold) bath. Thus, the collective double-bath effect measured by $\mathcal{K}(\tau) - \mathcal{K}_h(\tau) - \mathcal{K}_c(\tau)$ vanishes in the limit of weak system–bath coupling.

Equation (32) can be made Markovian if the time scale of the bath-induced relaxation dynamics is much slower than the memory time [i.e., the time scale on which $\mathcal{K}_h^{(2)}(\tau)$ and $\mathcal{K}_c^{(2)}(\tau)$ vanish]. This corresponds to substituting $\hat{\sigma}(t-\tau)$ with $e^{i\mathcal{L}_s\tau/\hbar}\hat{\sigma}(t)$ and setting the upper limit of the time integrals to infinity in Eq. (32), and leads to a *Markovian quantum master equation* of the following form:

$$\frac{d}{dt}\hat{\sigma}(t) = -\frac{i}{\hbar}\mathcal{L}_s\hat{\sigma}(t) - \left[\mathcal{D}_h^{(2)} + \mathcal{D}_c^{(2)}\right]\hat{\sigma}(t), \tag{33}$$

where

$$\begin{aligned}\mathcal{D}_h^{(2)} &= \frac{1}{\hbar^2}\int_0^\infty d\tau\mathrm{Tr}_h\left\{\mathcal{L}_{sh}e^{-i\mathcal{L}_h\tau/\hbar}e^{-i\mathcal{L}_s\tau/\hbar}\mathcal{L}_{sh}\hat{\rho}_{h,eq}e^{i\mathcal{L}_s\tau/\hbar}\right\},\\ \mathcal{D}_c^{(2)} &= \frac{1}{\hbar^2}\int_0^\infty d\tau\mathrm{Tr}_c\left\{\mathcal{L}_{sc}e^{-i\mathcal{L}_c\tau/\hbar}e^{-i\mathcal{L}_s\tau/\hbar}\mathcal{L}_{sc}\hat{\rho}_{c,eq}e^{i\mathcal{L}_s\tau/\hbar}\right\}.\end{aligned} \tag{34}$$

Casting Eq. (34) in terms of the eigen-basis of $\hat{H}_s$, $\hat{H}_s|j\rangle = E_j|j\rangle$, the system–bath coupling terms can be written in the following form:

$$\hat{H}_{sh} = \sum_{j,k}\hat{\Lambda}_{h,jk}|j\rangle\langle k|, \quad \hat{H}_{sc} = \sum_{j,k}\hat{\Lambda}_{c,jk}|j\rangle\langle k|, \tag{35}$$

where $\{\hat{\Lambda}_{h,jk}\}$ and $\{\hat{\Lambda}_{c,jk}\}$ are the hot bath and cold bath operators, respectively. Making the secular approximation,[61] the dynamics of the system's populations, $\{\sigma_{jj}(t)\}$, and coherences, $\{\sigma_{jk}(t)\}$ $(j \neq k)$, can be described by

$$\begin{aligned}\frac{d}{dt}\sigma_{jj}(t) &= -\sum_{l\neq j}k_{l\leftarrow j}\sigma_{jj}(t) + \sum_{l\neq j}k_{j\leftarrow l}\sigma_{ll}(t),\\ \frac{d}{dt}\sigma_{jk}(t) &= -(i\omega_{jk} + \gamma_{jk})\sigma_{jk}(t).\end{aligned} \tag{36}$$

Here, $\{k_{l\leftarrow j}\}$ and γ_{jk} are the population relaxation and dephasing rate constants, respectively, which consist of sums of hot and cold bath contributions,

$$k_{l\leftarrow j} = k_{l\leftarrow j}^h + k_{l\leftarrow j}^c, \quad \gamma_{jk} = \gamma_{jk}^h + \gamma_{jk}^c. \tag{37}$$

Here,

$$\begin{aligned}k_{l\leftarrow j}^h &= \frac{1}{\hbar^2}\tilde{C}_{jl,lj}^h(\omega_{jl}), \quad k_{l\leftarrow j}^c = \frac{1}{\hbar^2}\tilde{C}_{jl,lj}^c(\omega_{jl}),\\ \gamma_{jk}^h &= \frac{1}{2}\left(\sum_{l\neq j}k_{l\leftarrow j}^h + \sum_{l\neq k}k_{l\leftarrow k}^h\right) + \frac{1}{2\hbar^2}\left[\tilde{C}_{jj,jj}^h(0) + \tilde{C}_{kk,kk}^h(0)\right],\\ \gamma_{jk}^c &= \frac{1}{2}\left(\sum_{l\neq j}k_{l\leftarrow j}^c + \sum_{l\neq k}k_{l\leftarrow k}^c\right) + \frac{1}{2\hbar^2}\left[\tilde{C}_{jj,jj}^c(0) + \tilde{C}_{kk,kk}^c(0)\right].\end{aligned} \tag{38}$$

Here, $\hbar\omega_{jl} = E_j - E_l$, $k_{l\leftarrow j}^h/k_{j\leftarrow l}^h = e^{\beta_h\hbar\omega_{jl}}$, $k_{l\leftarrow j}^c/k_{j\leftarrow l}^c = e^{\beta_c\hbar\omega_{jl}}$, and

$$\begin{aligned}\tilde{C}_{jl,lj}^h(\omega_{jl}) &= \int_{-\infty}^\infty d\tau e^{i\omega_{jl}\tau}C_{jl,lj}^h(\tau),\\ C_{jl,lj}^h(\tau) &= \mathrm{Tr}_h\left[\hat{\rho}_h^{eq}e^{i\hat{H}_h\tau/\hbar}\hat{\Lambda}_{h,jl}e^{-i\hat{H}_h\tau/\hbar}\hat{\Lambda}_{h,lj}\right],\\ \tilde{C}_{jl,lj}^c(\omega_{jl}) &= \int_{-\infty}^\infty d\tau e^{i\omega_{jl}\tau}C_{jl,lj}^c(\tau),\\ C_{jl,lj}^c(\tau) &= \mathrm{Tr}_c\left[\hat{\rho}_c^{eq}e^{i\hat{H}_c\tau/\hbar}\hat{\Lambda}_{c,jl}e^{-i\hat{H}_c\tau/\hbar}\hat{\Lambda}_{c,lj}\right].\end{aligned} \tag{39}$$

In what follows, we will refer to the Markovian and secular quantum master equation in Eq. (36) as the *Redfield quantum master equation*. It should be noted that non-Markovian and/or nonsecular versions of the Redfield quantum master equation exist and

can, in some cases, improve their accuracy (as long as treating the system–bath coupling as a small perturbation within second-order time-dependent perturbation theory is valid). Our choice to focus on the Markovian and secular quantum master equation as a reference is motivated by the fact that it has the Lindblad form, which is widely used and guarantees complete positivity.[2,62] Deviations between the predictions of the Redfield quantum master equation and the GQME [Eq. (16)] will be used as a measure of the effect of strong coupling, non-Markovity, and non-secular terms.

It should be noted that several other approaches have been proposed in the past to account for strong system–bath coupling effects beyond second-order perturbation theory. One such approach is to extend the perturbation expansion to higher than second-order terms.[63–67] By incorporating higher than second-order terms, such an approach should be able to account for the non-additivity of the baths. However, the derivation and evaluation of higher-order terms become increasingly difficult and cumbersome as the order of the perturbation expansion increases. Furthermore, beyond a critical coupling strength, the perturbation approach has been observed to exhibit asymptotic divergence, such that including additional higher-order terms no longer improves the accuracy of the results.[10,68] Thus, such an approach would be limited by convergence and the order of the highest term in the perturbation expansion one can calculate in practice.

Another approach for going beyond conventional second-order perturbation theory employs the polaron transformation.[69,70] Combined with full-counting statistics, this approach can provide analytical heat current expressions for the nonequilibrium spin-boson model and recovers the Redfield and Fermi-golden-rule limits in the weak and strong coupling regimes, respectively.[69] However, this approach remains approximate and is generally limited to systems linearly coupled to harmonic baths.

In this work, the second-order perturbative treatment is employed to illustrate the non-additive effects of multiple baths. For regimes where perturbative approaches become inadequate, the GQME approach pursued here provides an inherently non-perturbative and general-purpose framework that captures system–bath coupling effects to infinite order.

III. A DEMONSTRATIVE APPLICATION TO A TWO-LEVEL SYSTEM LINEARLY COUPLED TO HOT AND COLD HARMONIC BATHS

A. Model Hamiltonian

In this section, we demonstrate the theoretical framework outlined in Sec. II and the insights that can be obtained from it on a benchmark model that consists of a two-level system linearly coupled to hot and cold harmonic baths. To this end, we adopted a model Hamiltonian previously studied by Song and Shi in Ref. 9, which has the form of Eq. (4), with $\{\hat{H}_s, \hat{H}_h, \hat{H}_c, \hat{H}_{sh}, \hat{H}_{sc}\}$ given by

$$\begin{aligned} \hat{H}_s &= \Delta\hat{\sigma}_x, \\ \hat{H}_h = \sum_{j=1}^{N}\left[\frac{\hat{P}_{hj}^2}{2} + \frac{\omega_{hj}^2\hat{R}_{hj}^2}{2}\right],\ \hat{H}_c &= \sum_{j=1}^{N}\left[\frac{\hat{P}_{cj}^2}{2} + \frac{\omega_{cj}^2\hat{R}_{cj}^2}{2}\right], \\ \hat{H}_{sh} = \sum_{j=1}^{N} c_{hj}\hat{R}_{hj}\hat{\sigma}_z,\ \hat{H}_{sc} &= \sum_{j=1}^{N} c_{cj}\hat{R}_{cj}\hat{\sigma}_z. \end{aligned} \tag{40}$$

TABLE I. Spin-boson model parameters.

Model no.	Δ	β_h	β_c	η_α	$\gamma_{\alpha,1}$	$\gamma_{\alpha,2}$	$\gamma_{\alpha,3}$
1	0.1	0.5	1.5	0.01	0.5	1.0	1.5
2	0.1	0.5	1.5	0.1	0.5	1.0	1.5
3	0.1	0.5	1.5	1.0	0.5	1.0	1.5
4	0.5	0.5	1.5	0.01	0.5	1.0	1.5
5	0.5	0.5	1.5	0.1	0.5	1.0	1.5
6	0.5	0.5	1.5	1.0	0.5	1.0	1.5

Here, $\hat{\sigma}_x = |0\rangle\langle 1| + |1\rangle\langle 0|$, $\hat{\sigma}_y = -i(|0\rangle\langle 1| - |1\rangle\langle 0|)$, and $\hat{\sigma}_z = |0\rangle\langle 0| - |1\rangle\langle 1|$ are the Pauli operators, with $|0\rangle$ and $|1\rangle$ corresponding to the eigen states of $\hat{\sigma}_z$ with eigenvalues $+1$ and -1, respectively; and $\{\hat{R}_{hj}, \hat{P}_{hj}, \omega_{hj}, c_{hj} | j = 1, \ldots, N\}$ and $\{\hat{R}_{cj}, \hat{P}_{cj}, \omega_{cj}, c_{cj} | j = 1, \ldots, N\}$ denote the mass-weighted coordinates, momenta, frequencies, and coupling coefficients of the hot and cold bath modes, respectively. It should be noted that for this model, the hot and cold baths' Hamiltonians are identical and coupled to the two-level system in the same way.

The values of $\{\omega_{hj}, c_{hj} | j = 1, \ldots, N\}$ and $\{\omega_{cj}, c_{cj} | j = 1, \ldots, N\}$ are extracted from spectral density functions, which are assumed to be identical for both baths and given by $(\alpha = h, c)$,[9]

$$\begin{aligned} I_\alpha(\omega) &= \frac{\pi}{2}\sum_{j=1}^{N}\frac{c_{\alpha j}^2}{\omega_{\alpha j}}\delta(\omega - \omega_{\alpha j}) \\ &= \frac{\eta_\alpha\omega\gamma_{\alpha,1}\gamma_{\alpha,2}\gamma_{\alpha,3}}{(\omega^2 + \gamma_{\alpha,1}^2)(\omega^2 + \gamma_{\alpha,2}^2)(\omega^2 + \gamma_{\alpha,3}^2)}. \end{aligned} \tag{41}$$

The initial state of the overall system is assumed to be given by Eq. (10), with $\hat{\sigma}(0) = |0\rangle\langle 0|$,

$$\hat{\rho}(0) = \hat{\rho}_h^{eq} \otimes \hat{\rho}_c^{eq} \otimes |0\rangle\langle 0|. \tag{42}$$

Here, $\hat{\rho}_h^{eq}$ and $\hat{\rho}_c^{eq}$ are defined as in Eq. (8).

Calculations were performed for six realizations of this model that correspond to the values of the parameters in Table I. The values of β_h, β_c, $\gamma_{\alpha,1}$, $\gamma_{\alpha,2}$, and $\gamma_{\alpha,3}$ are the same for all six models. The models differ with respect to the values of Δ ($\Delta = 0.1$ for models 1–3, while $\Delta = 0.5$ for models 4–6) and η_α ($\eta_\alpha = 0.01$ for models 1 and 4, $\eta_\alpha = 0.1$ for models 2 and 5, and $\eta_\alpha = 1.0$ for models 3 and 6). It should be noted that quantum-mechanically exact results obtained via the HEOM method were reported in Ref. 9 for models 2, 3, 5, and 6. Models 1 and 4 were added in this paper since they correspond to weaker system–bath coupling in order to demonstrate the more additive nature of the memory kernel in this case.

B. Computational details

Calculating the memory kernel, Eq. (17), for the GQME that describes the dynamics of the two-level system coupled to two baths, Eq. (16), requires solving the Volterra equation, Eq. (19), which requires $\mathcal{U}(\tau)$ as the PFI, Eq. (18). To this end, we calculated the 4×4 matrix that represents $\mathcal{U}(\tau)$ via the HEOM method (see the Appendix) and its time derivatives, $\dot{\mathcal{U}}(\tau)$ and $\ddot{\mathcal{U}}(\tau)$, via the finite central difference method available in the NumPy Python library. The Volterra equation was then solved numerically via the iterative

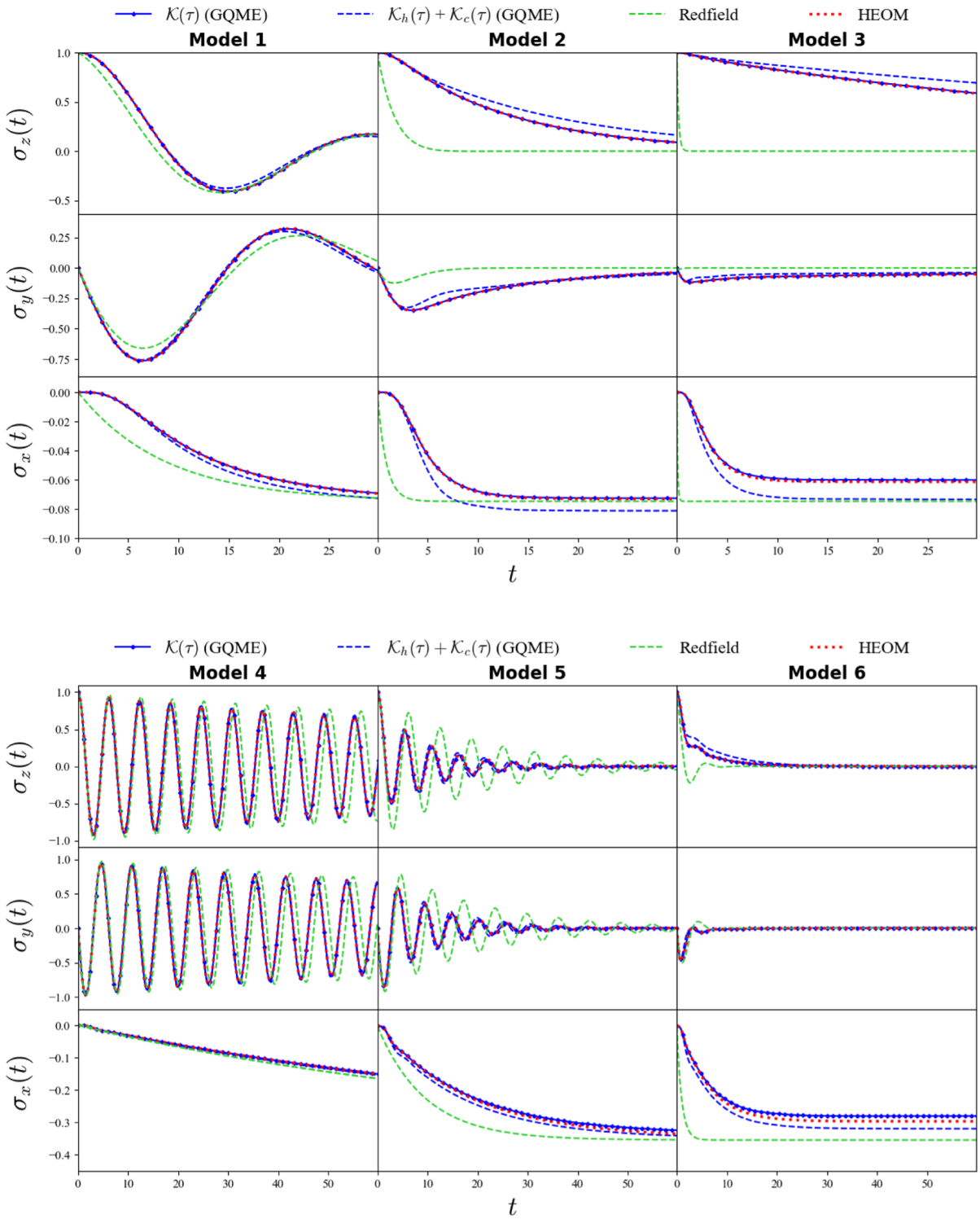

FIG. 1. $\sigma_x(t)$, $\sigma_y(t)$, and $\sigma_z(t)$ as a function of time for models 1–3 (top panel) and models 4–6 (bottom panel) in Table I. Shown are exact HEOM-based results (dotted red line), GQME-based results with the exact memory kernel $\mathcal{K}(\tau)$, Eq. (17), calculated from HEOM-based PFIs (solid blue line), GQME-based results with the approximate additive memory kernel $\mathcal{K}_h(\tau) + \mathcal{K}_c(\tau)$, Eqs. (25) and (28), calculated from HEOM-based PFIs (dashed blue line), and results based on the Markovian and secular Redfield quantum master equation, Eq. (36) (dashed green line).

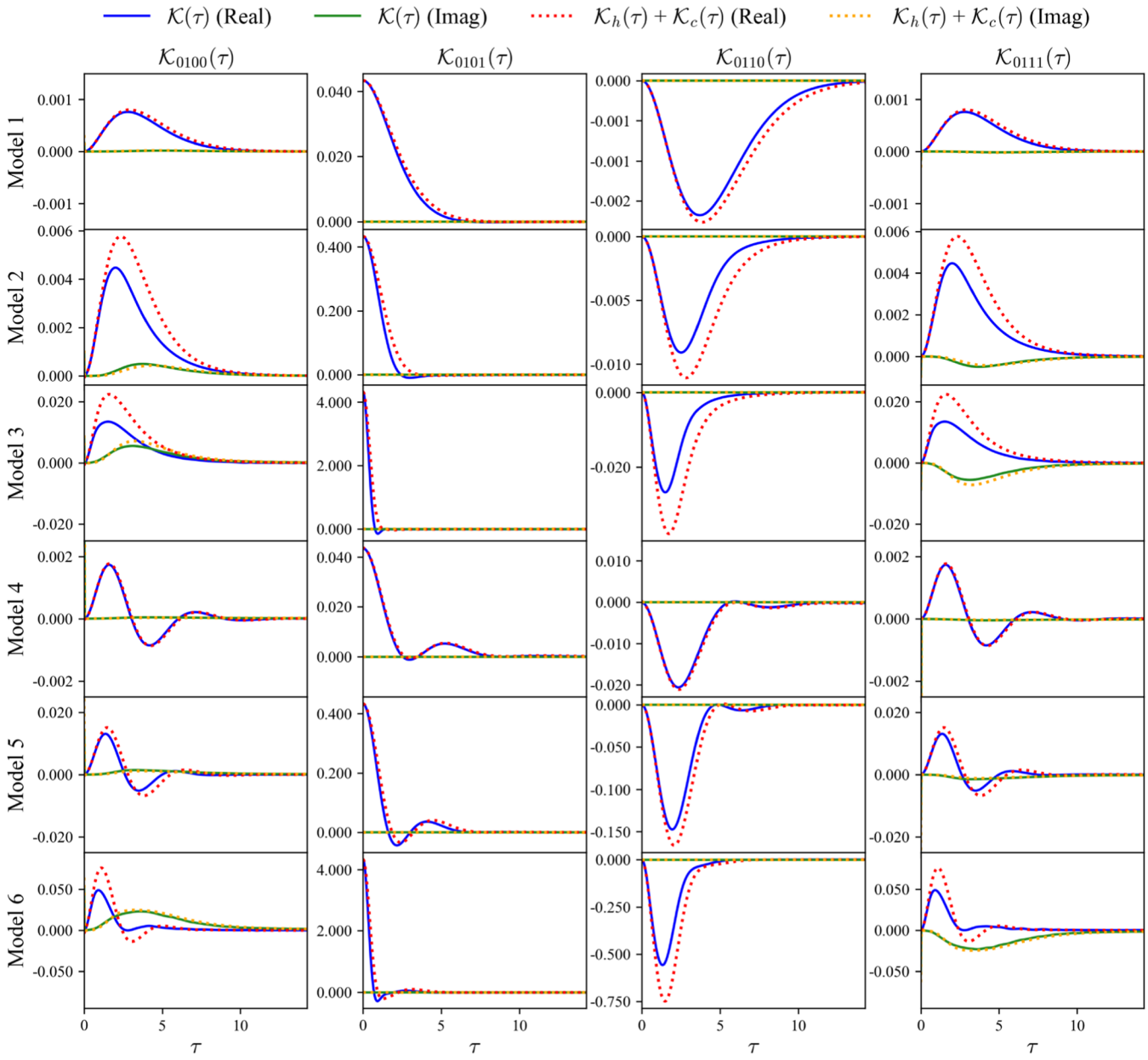

FIG. 2. A comparison of the four independent and non-vanishing matrix elements $[(01,00),(01,01),(01,10),(01,11)]$ of $\mathcal{K}(\tau)$ vs $\mathcal{K}_h(\tau) + \mathcal{K}_c(\tau)$ for the six spin-boson models under consideration. Shown are the real (solid blue line) and imaginary (solid green line) parts of $\mathcal{K}(\tau)$ vs the real (dashed red line) and imaginary (dashed orange line) parts of $\mathcal{K}_h(\tau) + \mathcal{K}_c(\tau)$.

algorithm outlined in Refs. 44 and 71, followed by propagation of the GQME using a fourth-order Runge–Kutta method.

It should be noted that while the results are presented in terms of the eigen-basis of $\hat{\sigma}_z$ ($\{|0\rangle, |1\rangle\}$, such that $\hat{\sigma}_z|0\rangle = |0\rangle$ and $\hat{\sigma}_z|1\rangle = -|1\rangle$), the Redfield quantum master equation, Eq. (36), is given in terms of the eigen-basis of $\hat{\sigma}_x$ (since the system Hamiltonian in this case is given by $\hat{H}_s = \Delta\hat{\sigma}_x$).

C. Results and discussion

We start by demonstrating the effect of the system–bath coupling on the dynamics of the system. To this end, we compare and contrast the dynamics of the three components of the Bloch vector, $[\sigma_x(t), \sigma_y(t), \sigma_z(t)]$, where $\sigma_u(t) = \langle\hat{\sigma}_u\rangle(t)$, as obtained in three different ways: (1) The GQME, Eq. (16), with the *exact two-bath memory kernel*, Eq. (17); (2) the GQME, Eq. (16), with the *sum of*

exact single-bath memory kernels, $\mathcal{K}(\tau) \approx \mathcal{K}_h(\tau) + \mathcal{K}_c(\tau)$, Eqs. (25) and (28); and (3) the *secular and Markovian Redfield quantum master equation*, Eq. (36). The results of this comparison for models 1–6 are shown in Fig. 1.

We first note that the dynamics generated via the GQME with the HEOM-based exact memory kernel coincides with that obtained via direct use of the HEOM method. This is to be expected since, given the exact memory kernel, the GQME is the exact equation of motion for the system's density matrix.

In addition, as expected, the dynamics of σ_x (which correspond to energy relaxation) is seen to become increasingly more damped with increasing η_α, while the dynamics of σ_y and σ_z

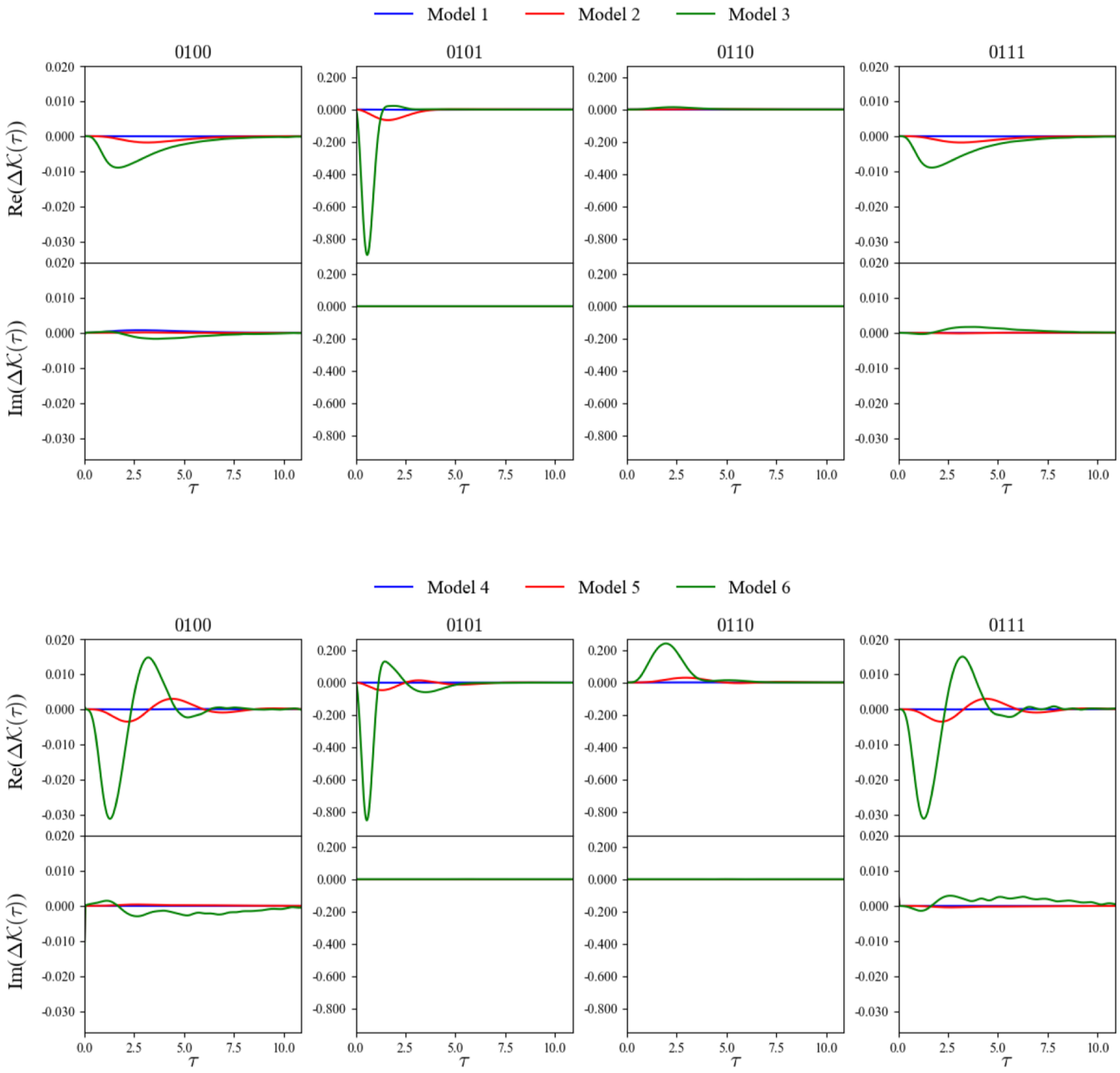

FIG. 3. The real (top panels) and imaginary (lower panels) parts of the (01, 00), (01, 01), (01, 10), and (01, 11) nonvanishing matrix elements of $\Delta\mathcal{K}(\tau) = \mathcal{K}(\tau) - \mathcal{K}_h(\tau) - \mathcal{K}_c(\tau)$ for the six spin-boson models under consideration.

(which correspond to phase damping) is seen to go from under-damped to over-damped with increasing η_α. It should also be noted that while σ_y and σ_z are seen to vanish at steady state regardless of the value of η_α, the steady state value of σ_x is non-zero and strongly dependent on η_α. As η_α increases, the steady state value of σ_x is also seen to deviate more and more from the value predicted by the Redfield quantum master equation.

The increasing non-additivity of the memory kernel with increasing system–bath coupling strength (as measured by η_α) is manifested by the growing difference between the exact results and the results obtained by using the approximation $\mathcal{K}(\tau) \approx \mathcal{K}_h(\tau) + \mathcal{K}_c(\tau)$. The non-additive nature of the bath-induced effect is more pronounced for models 1–3 than for models 4–6. This behavior can be traced back to the increasing role of coherent Hamiltonian dynamics relative to dissipative dynamics with increasing Δ.

From the three components of the Bloch vector, σ_x and σ_z are seen to be more sensitive than σ_y to the non-additive nature of the bath-induced effect. This sensitivity manifests itself both in the transient dynamics and steady-state values and can be traced back to the fact that the Hamiltonian in Eq. (40) is given in terms of $\hat{\sigma}_x$ and $\hat{\sigma}_z$, but not $\hat{\sigma}_y$.

Finally, while the dynamics generated by the secular and Markovian Redfield quantum master equation is seen to get closer to the exact dynamics with decreasing η_α, deviations are still observable even at the weakest system–bath coupling under consideration ($\eta_\alpha = 0.01$). Those deviations are particularly manifest for σ_x in model 1, where they can be traced back to transient non-Markovian effects. In particular, the onset of Markovian dynamics in this case occurs at $t \sim 5$, as opposed to at the initial time (as required by the assumption of Markovity). Thus, while the dynamics at $t > 5$ is exponential and parallels the exact dynamics, the delayed onset of Markovian dynamics leads to the observed deviation.

Further insight into the non-additivity of the bath-induced effect can be obtained by directly comparing $\mathcal{K}(\tau)$ with $\mathcal{K}_h(\tau) + \mathcal{K}_c(\tau)$. To this end, it should be remembered that $\mathcal{K}(\tau)$, $\mathcal{K}_h(\tau)$, and $\mathcal{K}_c(\tau)$ are superoperators and, therefore, representable in terms of $n^2 \times n^2$ matrices [see Eq. (22)]. For the spin-boson model under consideration, $n = 2$, which means that $\mathcal{K}(\tau)$, $\mathcal{K}_h(\tau)$, and $\mathcal{K}_c(\tau)$ are representable in terms of 4×4 matrices. However, represented in terms of the $\hat{\sigma}_z$ eigen-basis, $\{|0\rangle, |1\rangle\}$, the (jj, lm) matrix elements of $\mathcal{K}(\tau)$, $\mathcal{K}_h(\tau)$, and $\mathcal{K}_c(\tau)$ vanish for the spin-boson model.[44,72] Thus, eight of the sixteen matrix elements of $\mathcal{K}(\tau)$, $\mathcal{K}_h(\tau)$, and $\mathcal{K}_c(\tau)$ vanish (i.e., the ones for which $jj = 00, 11$ and $lm = 00, 01, 10, 11$).[44,72] For the remaining eight non-vanishing matrix elements, four can be shown to be the complex conjugates of the other four, since $\mathcal{K}_{jk,lm}(\tau) = \mathcal{K}^*_{kj,ml}(\tau)$, which means that the memory kernels can be determined by the values of the following four matrix elements: $\{\mathcal{K}_{0100}(\tau), \mathcal{K}_{0101}(\tau), \mathcal{K}_{0110}(\tau), \mathcal{K}_{0111}(\tau)\}$.[44,72]

A comparison of the aforementioned four independent and non-vanishing matrix elements of $\mathcal{K}(\tau)$ vs $\mathcal{K}_h(\tau) + \mathcal{K}_c(\tau)$ is shown in Fig. 2 for the six spin-boson models under consideration (see Table I). The corresponding real and imaginary parts of the (01, 00), (01, 01), (01, 10), and (01, 11) matrix elements of $\mathcal{K}(\tau) - \mathcal{K}_h(\tau) - \mathcal{K}_c(\tau)$ are shown in Fig. 3.

The difference between $\mathcal{K}(\tau)$ and $\mathcal{K}_h(\tau) + \mathcal{K}_c(\tau)$ is seen to increase with increasing coupling strength between the system and the baths, as measured by η_α. In particular, $\mathcal{K}_h(\tau) + \mathcal{K}_c(\tau)$ is seen to reproduce $\mathcal{K}(\tau)$ rather well when $\eta_\alpha = 0.01$ (models 1 and 4), which is consistent with the expectation that the memory kernel becomes additive in the limit of weak system–bath coupling [see Eq. (30)]. However, the effect of the baths becomes increasingly non-additive as η_α increases, as is clearly evident from the growing deviation between $\mathcal{K}(\tau)$ and $\mathcal{K}_h(\tau) + \mathcal{K}_c(\tau)$ as η_α is increased.

Interestingly, the non-additive nature of $\mathcal{K}(\tau)$ is dependent on the matrix element. In particular, while $\mathcal{K}_{0101}(\tau)$ is well approximated by $\mathcal{K}_{h,0101}(\tau) + \mathcal{K}_{c,0101}(\tau)$, this is not the case for $\mathcal{K}_{0100}(\tau)$, $\mathcal{K}_{0111}(\tau)$, and $\mathcal{K}_{0110}(\tau)$. It should, however, be noted that the absolute error associated with assuming additivity is actually similar for all four matrix elements (see Fig. 3). However, this absolute error translates into a much smaller relative error in the case of $\mathcal{K}_{0101}(\tau)$, because it is so much larger than $\mathcal{K}_{0100}(\tau)$, $\mathcal{K}_{0111}(\tau)$, and $\mathcal{K}_{0110}(\tau)$.

It should be noted that $\mathcal{K}_{0101}(\tau)$ couples σ_{10} with itself. This term, therefore, gives rise to coherence damping in the $\{|0\rangle, |1\rangle\}$ representation. Thus, the fact that $\mathcal{K}_{0101}(\tau)$ can be well approximated as additive implies that this coherence damping process is relatively insensitive to the non-additive nature of the effects of the baths. In contrast, $\mathcal{K}_{0100}(\tau)$ and $\mathcal{K}_{0111}(\tau)$ give rise to bath-induced coupling between populations and coherences in the $\{|0\rangle, |1\rangle\}$ representation, which can give rise to population-to-coherence and coherence-to-population transfer. Similarly, $\mathcal{K}_{0110}(\tau)$ gives rise to bath-induced coupling between different coherences, which can lead to coherence transfer.

Thus, unlike coherence damping, population-to-coherence, coherence-to-population, and coherence-to-coherence transfer are seen to become strongly non-additive with increasing system–bath coupling. This is consistent with the fact that the emergence of those processes as non-negligible beyond the limit of weak system–bath coupling goes hand in hand with their non-additive nature as signatures of strong system–bath coupling.

IV. CONCLUDING REMARKS

The non-additivity of the memory kernel, as measured by the difference between $\mathcal{K}(\tau)$ and $\mathcal{K}_h(\tau) + \mathcal{K}_c(\tau)$, can serve as a test for the adequacy of methods that treat system–bath coupling as a weak perturbation. Generally speaking, $\mathcal{K}(\tau)$ can only be written in the additive form $\mathcal{K}_h(\tau) + \mathcal{K}_c(\tau)$ under weak system–bath coupling conditions. Beyond that, the difference between $\mathcal{K}(\tau)$ and $\mathcal{K}_h(\tau) + \mathcal{K}_c(\tau)$ grows with the strength of system–bath coupling. This happens because the effect of the bath on a system is *non-local*. In other words, *the cumulative effect of coupling to multiple baths is not the same as the sum of the effects of the individual baths.*

The effect of non-additivity depends on the matrix element of $\mathcal{K}(\tau)$. In particular, the *relative* error associated with approximating $\mathcal{K}_{jkmn}(\tau)$ by $\mathcal{K}_{h,jkmn}(\tau) + \mathcal{K}_{c,jkmn}(\tau)$ depends on (jk, mn), which in turn correspond to the dynamical coupling between $\sigma_{jk}(t)$ and $\sigma_{mn}(t)$. For example, we have shown that for the spin-boson models under consideration in this paper, coherence damping, which is associated with $\mathcal{K}_{0101}(\tau)$, is well approximated by

$\mathcal{K}_{h,0101}(\tau) + \mathcal{K}_{c,0101}(\tau)$, while coherence-to-coherence, coherence-to-population, and population-to-coherence transfer, associated with $\mathcal{K}_{0110}(\tau)$, $\mathcal{K}_{0100}(\tau)$, and $\mathcal{K}_{0111}(\tau)$, show strong non-additive behavior. Thus, non-additivity is process-dependent.

The fact that the memory kernel becomes non-additive beyond the limit of weak system–bath coupling also suggests that it may not be possible to break down the heat flow between the system and the baths into a sum of heat flows between the system and the individual baths. More specifically, defining the energy of the system as the expectation value of $\hat{H}_s$ at time t, $\langle \hat{H}_s \rangle(t)$, it can be shown that

$$\begin{aligned} \frac{d}{dt}\langle \hat{H}_s \rangle &= \mathrm{Tr}_s\left[\hat{H}_s \frac{d}{dt}\hat{\sigma}(t)\right] \\ &= -\int_0^t d\tau \mathrm{Tr}_s\left[\hat{H}_s \mathcal{K}(\tau)\hat{\sigma}(t-\tau)\right], \end{aligned} \tag{43}$$

where we used the fact that $\mathrm{Tr}_s[\hat{H}_s(t)\mathcal{L}_s\hat{\sigma}(t)] = 0$. According to Eq. (43), the only way for the energy of the system to change is by exchanging energy with the heat baths. It, therefore, seems reasonable to identify $d\langle \hat{H}_s \rangle/dt$ as the *overall* heat flow between the system and the baths, which we will denote $\dot{Q}$. Thus, $\dot{Q} = d\langle \hat{H}_s \rangle/dt$, such that $\dot{Q} > 0$ means heat transfer from the baths into the system and $\dot{Q} < 0$ means heat transfer from the system into the baths. It should also be noted that $\dot{Q} = 0$ at steady state.

Now, if $\mathcal{K}(\tau)$ is additive, namely, $\mathcal{K}(\tau) = \mathcal{K}_h(\tau) + \mathcal{K}_c(\tau)$, then $\dot{Q}$ is also additive, such that $\dot{Q} = \dot{Q}_h + \dot{Q}_c$, where $\dot{Q}_h$ and $\dot{Q}_c$ are the heat flows between the system and the hot and cold baths, respectively,

$$\begin{aligned} \dot{Q}_h &= -\int_0^t d\tau \mathrm{Tr}_s\left[\hat{H}_s \mathcal{K}_h(\tau)\hat{\sigma}(t-\tau)\right], \\ \dot{Q}_c &= -\int_0^t d\tau \mathrm{Tr}_s\left[\hat{H}_s \mathcal{K}_c(\tau)\hat{\sigma}(t-\tau)\right]. \end{aligned} \tag{44}$$

However, $\mathcal{K}(\tau) = \mathcal{K}_h(\tau) + \mathcal{K}_c(\tau)$ only holds in the limit of weak system–bath coupling. Thus, there seems to be no clear way to define $\dot{Q}_h$ and $\dot{Q}_c$ beyond this limit. Indeed, previous studies of systems coupled to multiple baths found that different definitions for $\dot{Q}_h$ and $\dot{Q}_c$ gave rise to different results beyond the limit of weak system–bath coupling.[9]

The origin for the lack of consistent definitions for $\dot{Q}_h$ and $\dot{Q}_c$ can be traced back to the fact that the energy of the overall system includes the expectation values of the system–bath coupling terms $\langle \hat{H}_{sh} \rangle + \langle \hat{H}_{sc} \rangle$. Only in the limit of weak system–bath coupling do those terms become negligible, such that $d\langle H_s \rangle/dt + d\langle H_h \rangle/dt + d\langle H_c \rangle/dt = 0$, with $\dot{Q}_h = -d\langle H_h \rangle/dt$ and $\dot{Q}_c = -d\langle H_c \rangle/dt$. Beyond weak system–bath coupling, $d\langle \hat{H}_s \rangle/dt + d\langle \hat{H}_h \rangle/dt + d\langle \hat{H}_c \rangle/dt = -d\langle \hat{H}_{sh} \rangle/dt - d\langle \hat{H}_{sc} \rangle/dt$. Since $\langle \hat{H}_{sh} \rangle$ and $\langle \hat{H}_{sc} \rangle$ cannot be identified as purely system or bath observables, there appears to be no obvious way of identifying them as contributions to the energies of the system or the baths, which gives rise to an inherent ambiguity in the definitions of $\dot{Q}_h$ and $\dot{Q}_c$.

Similar non-additive effects were also reported by Hsieh *et al.*[70] and Wang *et al.*[69] by applying the polaron transformation to the nonequilibrium spin-boson model. Their studies showed that higher-order multi-boson processes involving correlated interactions between different baths can give rise to non-additive heat transport, highlighting the importance of cross-bath effects in determining the heat current.

The analysis presented in this paper demonstrates the usefulness of the GQME formalism as a way of quantifying non-additive and non-local effects and elucidating their signature on the system dynamics. Another advantage of the GQME approach is that it is not restricted to exact quantum methods such as HEOM and can be used with semiclassical and mixed quantum-classical methods for calculating the PFIs.[29,44,45,47] This in turn opens the door for applications to anharmonic all-atom models of complex molecular systems. Yet another advantage of the GQME approach is that it is flexible with respect to the projection operator used and, therefore, the dynamical quantity of interest.[59] For example, one can derive the GQME for only the populations (the diagonal elements of $\hat{\sigma}$), only the coherences (the off-diagonal elements of $\hat{\sigma}$), or more generally, any subset of $\hat{\sigma}$ matrix elements. For each of those choices, there would be a separate GQME with its own memory kernel. The extent of non-additivity can, therefore, depend on the choice of quantity of interest and the memory kernel that comes with it. Other possible extensions correspond to models where there are more than two baths, the bath and system–bath coupling differ from one bath to another,[17] and the baths start out in nonequilibrium states or entangled with the system. Work on such extensions is currently underway and will be reported in future publications.

ACKNOWLEDGMENTS

E.G. acknowledges the support from the NSF under Grant No. CHE 2154114.

AUTHOR DECLARATIONS

Conflict of Interest

The authors have no conflicts to disclose.

Author Contributions

Callie Wilson and Xiaohan Dan contributed equally to this work.

Callie Wilson: Conceptualization (equal); Data curation (lead); Formal analysis (lead); Investigation (equal); Methodology (equal); Software (equal); Validation (equal); Visualization (lead); Writing – original draft (lead); Writing – review & editing (equal). **Xiaohan Dan**: Conceptualization (equal); Data curation (equal); Formal analysis (equal); Investigation (equal); Methodology (equal); Software (equal); Validation (equal); Visualization (supporting); Writing – review & editing (equal). **Victor S. Batista**: Conceptualization (equal); Funding acquisition (equal); Methodology (equal); Project administration (equal); Resources (equal); Supervision (equal); Writing – review & editing (equal). **Eitan Geva**: Conceptualization (equal); Formal analysis (lead); Funding acquisition (equal); Investigation (equal); Methodology (equal); Project administration (equal); Resources (equal); Supervision (equal); Validation (equal);

Visualization (supporting); Writing – original draft (lead); Writing – review & editing (equal).

DATA AVAILABILITY

The data that support the findings of this study are available within the article.

APPENDIX: CALCULATION OF THE PFIs VIA THE HIERARCHICAL EQUATIONS OF MOTION METHOD

Calculating the memory kernel via Eq. (19) requires knowledge of $\mathcal{U}(t)$ as input. The quantity $\mathcal{U}(t)$ represents the mapping of the reduced system density matrix from time 0 to t, and its evaluation, therefore, requires propagating the open system dynamics.

Various methods have been developed for simulating open quantum dynamics. In this work, we employ the numerically exact HEOM method,[54–57] which has been widely applied to problems including charge and energy transfer, proton transfer, charge and heat transport through molecular junctions, and nonadiabatic surface scattering.[9–11,73–77]

Below, we briefly present the HEOM formalism for systems coupled to multiple baths relevant to the present work. More detailed derivations and discussions can be found in Ref. 9.

We start with the spin-boson Hamiltonian as defined in Eq. (40) and spectral densities as defined in Eq. (41). We then define the bath correlation function,[78–80]

$$C_\alpha(t) = \frac{1}{\pi}\int_0^\infty d\omega\, I_\alpha(\omega)\left[\coth\left(\frac{\beta_\alpha\hbar\omega}{2}\right)\cos(\omega t) - i\sin(\omega t)\right], \quad \text{(A1)}$$

with $\alpha = h, c$, and $I_\alpha(\omega)$ being the α-th bath spectral density [see Eq. (41)].

The HEOM approach is based on decomposing the bath correlation function into a sum of exponentials (which are known as *effective modes*),

$$C_\alpha(t) = \sum_k^K d_{\alpha k} e^{-v_{\alpha k} t}, \quad \text{(A2)}$$

where $v_{\alpha k}$ and $d_{\alpha k}$ are the frequencies and coefficients of the effective modes, respectively.

For the spectral density in Eq. (41), the coefficients $v_{\alpha,k}$ and $d_{\alpha,k}$ can be obtained analytically using the residue theorem. For the poles originating from the spectral density itself $(k = 1, 2, 3)$, one obtains

$$v_{\alpha,k} = \gamma_{\alpha,k}, \qquad k = 1, 2, 3, \quad \text{(A3)}$$

$$d_{\alpha,k} = \frac{\eta_\alpha}{2}\left[\cot\left(\frac{\beta_\alpha\hbar\gamma_{\alpha,k}}{2}\right) - i\right]\frac{\gamma_{\alpha,1}\gamma_{\alpha,2}\gamma_{\alpha,3}}{\prod_{j\neq k}(\gamma_{\alpha,j}^2 - \gamma_{\alpha,k}^2)}, \qquad k = 1, 2, 3. \quad \text{(A4)}$$

The finite temperature further introduces Matsubara contributions $(k \geq 4)$, given by

$$v_{\alpha,k} = \frac{2\pi(k-3)}{\beta_\alpha\hbar}, \qquad k \geq 4, \quad \text{(A5)}$$

$$d_{\alpha,k} = -\frac{2\eta_\alpha}{\beta_\alpha\hbar}\, v_{\alpha,k}\frac{\gamma_{\alpha,1}\gamma_{\alpha,2}\gamma_{\alpha,3}}{\prod_{m=1}^3(\gamma_{\alpha,m}^2 - v_{\alpha,k}^2)}, \qquad k \geq 4. \quad \text{(A6)}$$

Given the decomposition in Eq. (A2), the HEOM can be cast in the following form:[9,81]

$$\frac{\partial}{\partial t}\hat\rho_{\mathbf{n}}(t) = -\left(\frac{i}{\hbar}\mathcal{L}_s + \sum_{\alpha k} n_{\alpha k} v_{\alpha k}\right)\hat\rho_{\mathbf{n}}(t) - i\sum_{\alpha k}\left[\hat\sigma_z, \hat\rho_{\mathbf{n}_{\alpha k}^+}(t)\right] - \frac{i}{\hbar}\sum_{\alpha k} n_{\alpha k}\left(d_{\alpha k}\hat\sigma_z\hat\rho_{\mathbf{n}_{\alpha k}^-}(t) - \tilde d_{\alpha k}^*\hat\rho_{\mathbf{n}_{\alpha k}^-}(t)\hat\sigma_z\right), \quad \text{(A7)}$$

where $\mathcal{L}_s\hat\rho_{\mathbf{n}} = [\hat H_s, \hat\rho_{\mathbf{n}}]$. The auxiliary density operators (ADOs) $\hat\rho_{\mathbf{n}}$ have the same dimensionality as the system reduced density operator, with the multi-index $\mathbf{n} = \{n_1, \ldots, n_{\alpha k}, \ldots\}$, where $n_{\alpha k}$ is a non-negative integer characterizing the excitation number of the corresponding effective mode. When all $n_{\alpha k} = 0$, the zeroth-tier ADO $\hat\rho_{\mathbf{0}} \equiv \hat\sigma$ corresponds to the reduced density operator of interest.

For a given $\hat\rho_{\mathbf{n}}$, the tier is defined as $L = \sum_{\alpha,k} n_{\alpha k}$. The equation of motion of an L-tier ADO couples it to $(L+1)$-tier ADOs $\hat\rho_{\mathbf{n}_k^+}$ and $(L-1)$-tier ADOs $\hat\rho_{\mathbf{n}_k^-}$, where $\mathbf{n}_{\alpha k}^+ = \{n_1, \ldots, n_{\alpha k} + 1, \cdots\}$ and $\mathbf{n}_{\alpha k}^- = \{n_1, \ldots, n_{\alpha k} - 1, \cdots\}$. This hierarchical structure across different tiers defines the HEOM.

In numerical calculations, the hierarchy is truncated by systematically increasing the effective mode cutoff K and the maximum tier L until convergence of the dynamics is reached. In particular, for the parameters listed in Table I, convergence is achieved by retaining one Matsubara term per bath $(K = 4)$, while truncating the effective mode occupation numbers $n_{\alpha,k}$ at 45. The HEOM is propagated using the mpsqd[82] package based on the matrix product state (MPS) technique, with a bond dimension of 50. Further technical details of the MPS-HEOM implementation can be found in Ref. 82.

REFERENCES

[1] A. G. Redfield, "On the theory of relaxation processes," IBM J. Res. Dev. **1**, 19 (1957).
[2] R. Alicki and K. Lendi, *Quantum Dynamical Semigroups and Applications* (Springer-Verlag, Berlin, 1987).
[3] W. T. Pollard, A. K. Felts, and R. A. Friesner, "The Redfield equation in condensed-phase quantum dynamics," Adv. Chem. Phys. **93**, 77 (1996).
[4] R. Zwanzig, *Nonequilibrium Statistical Mechanics* (Oxford University Press, New York, 2001).
[5] Q. Shi and E. Geva, "A new approach to calculating the memory kernel of the generalized quantum master equation for an arbitrary system-bath coupling," J. Chem. Phys. **119**, 12063–12076 (2003).
[6] H. Breuer and F. Petruccione, *The Theory of Open Quantum Systems* (Oxford University Press, New York, 2006).
[7] E. Geva and R. Kosloff, "Three-level quantum amplifier as a heat engine: A study in finite-time thermodynamics," Phys. Rev. E **49**, 3903 (1994).
[8] E. Geva and R. Kosloff, "The quantum heat engine and heat pump: An irreversible thermodynamic analysis of the three-level amplifier," J. Chem. Phys. **104**, 7681 (1996).
[9] L. Song and Q. Shi, "Hierarchical equations of motion method applied to nonequilibrium heat transport in model molecular junctions: Transient heat current and high-order moments of the current operator," Phys. Rev. B **95**, 064308 (2017).
[10] X. Dan, M. Xu, Y. Yan, and Q. Shi, "Generalized master equation for charge transport in a molecular junction: Exact memory kernels and their high order expansion," J. Chem. Phys. **156**, 134114 (2022).
[11] X. Dan, M. Xu, J. T. Stockburger, J. Ankerhold, and Q. Shi, "Efficient low-temperature simulations for fermionic reservoirs with the hierarchical equations of motion method: Application to the Anderson impurity model," Phys. Rev. B **107**, 195429 (2023).

[12]D. Segal and A. Nitzan, "Spin-boson thermal rectifier," Phys. Rev. Lett. **94**, 034301 (2005).
[13]D. Segal and A. Nitzan, "Heat rectification in molecular junctions," J. Chem. Phys. **122**, 194704 (2005).
[14]K. Saito and T. Kato, "Kondo signature in heat transfer via a local two-state system," Phys. Rev. Lett. **111**, 214301 (2013).
[15]D. Segal, "Heat transfer in the spin-boson model: A comparative study in the incoherent tunneling regime," Phys. Rev. E **90**, 012148 (2014).
[16]M. J. Martínez-Pérez, A. Fornieri, and F. Giazotto, "Rectification of electronic heat current by a hybrid thermal diode," Nat. Nanotechnol. **10**, 303–307 (2015).
[17]C. Duan, C.-Y. Hsieh, J. Liu, J. Wu, and J. Cao, "Unusual transport properties with noncommutative system–bath coupling operators," J. Phys. Chem. Lett. **11**, 4080–4085 (2020).
[18]N. Anto-Sztricaks, F. Ivander, and D. Segal, "Quantum thermal transport beyond second order with the reaction coordinate mapping," J. Chem. Phys. **156**, 214107 (2022).
[19]N. Anto-Sztricaks, A. Nazir, and D. Segal, "Effective-Hamiltonian theory of open quantum systems at strong coupling," PRX Quantum **4**, 020307 (2023).
[20]L. Li and X. Cao, "Coherent destruction of tunneling of quantum energy transport in a driven nonequilibrium spin-boson model," Phys. Rev. B **110**, 075403 (2024).
[21]J. Garwoła and D. Segal, "Open quantum systems with noncommuting coupling operators: An analytic approach," Phys. Rev. B **110**, 174304 (2024).
[22]J. Chen, J. Grawola, and D. Segal, "Suppression of decoherence dynamics by a dissipative bath at strong coupling," Phys. Rev. A **112**, 022209 (2025).
[23]M. Naher, D. C. Milan, O. A. Al-Owaedi, I. J. Planje, S. Bock, J. Hurtado-Gallego, P. Bastante, Z. M. Abd Dawood, L. Rincón-García, G. Rubio-Bollinger, S. J. Higgins, N. Agraït, C. J. Lambert, R. J. Nichols, and P. Low, "Molecular structure(thermo)electric property relationships in single-molecule junctions and comparisons with single- and multiple-parameter models," J. Am. Chem. Soc. **143**, 3817–3829 (2021).
[24]N. Boujada and D. Segal, "From dissipative dynamics to studies of heat transfer at the nanoscale: Analysis of the spin-boson model," J. Phys. Chem. A **118**, 11323–11336 (2014).
[25]H. B. Callen, *Thermodynamics* (John Wiley, New York, 1979).
[26]F. Binder, L. A. Correa, C. Gogolin, J. Anders, and G. Adesso, *Thermodynamics in the Quantum Regime: Fundamental Aspects and New Directions* (Springer, Cham, 2018).
[27]S. Nakajima, "On the quantum theory of transport phenomena," Prog. Theor. Phys. **20**, 948–959 (1958).
[28]R. Zwanzig, "Ensemble method in the theory of irreversibility," J. Chem. Phys. **33**, 1338–1341 (1960).
[29]Q. Shi and E. Geva, "A semiclassical generalized quantum master equation for an arbitrary system-bath coupling," J. Chem. Phys. **120**, 10647–10658 (2004).
[30]M.-L. Zhang, B. J. Ka, and E. Geva, "Nonequilibrium quantum dynamics in the condensed phase via the generalized quantum master equation," J. Chem. Phys. **125**, 044106 (2006).
[31]B. J. Ka, M.-L. Zhang, and E. Geva, "Homogeneity and Markovity of electronic dephasing in liquid solutions," J. Chem. Phys. **125**, 124509 (2006).
[32]G. Cohen and E. Rabani, "Memory effects in nonequilibrium quantum impurity models," Phys. Rev. B **84**, 075150 (2011).
[33]E. Y. Wilner, H. Wang, G. Cohen, M. Thoss, and E. Rabani, "Bistability in a nonequilibrium quantum system with electron-phonon interactions," Phys. Rev. B **88**, 045137 (2013).
[34]G. Cohen, E. Y. Wilner, and E. Rabani, "Generalized projected dynamics for non-system observables of non-equilibrium quantum impurity models," New J. Phys. **15**, 073018 (2013).
[35]G. Cohen, E. Gull, D. R. Reichman, A. J. Millis, and E. Rabani, "Numerically exact long-time magnetization dynamics at the nonequilibrium Kondo crossover of the Anderson impurity model," Phys. Rev. B **87**, 195108 (2013).
[36]A. Kelly and T. E. Markland, "Efficient and accurate surface hopping for long time nonadiabatic quantum dynamics," J. Chem. Phys. **139**, 014104 (2013).
[37]L. Kidon, E. Y. Wilner, and E. Rabani, "Exact calculation of the time convolutionless master equation generator: Application to the nonequilibrium resonant level model," J. Chem. Phys. **143**, 234110 (2015).
[38]W. C. Pfalzgraff, A. Kelly, and T. E. Markland, "Nonadiabatic dynamics in atomistic environments: Harnessing quantum-classical theory with generalized quantum master equations," J. Phys. Chem. Lett. **6**, 4743–4748 (2015).
[39]A. Montoya-Castillo and D. R. Reichman, "Approximate but accurate quantum dynamics from the Mori formalism: I. Nonequilibrium dynamics," J. Chem. Phys. **144**, 184104 (2016).
[40]A. Kelly, N. Brackbill, and T. E. Markland, "Accurate nonadiabatic quantum dynamics on the cheap: Making the most of mean field theory with master equations," J. Chem. Phys. **142**, 094110 (2015).
[41]A. Kelly, A. Montoya-Castillo, L. Wang, and T. E. Markland, "Generalized quantum master equations in and out of equilibrium: When can one win?," J. Chem. Phys. **144**, 184105 (2016).
[42]L. Kidon, H. Wang, M. Thoss, and E. Rabani, "On the memory kernel and the reduced system propagator," J. Chem. Phys. **149**, 104105 (2018).
[43]W. C. Pfalzgraff, A. Montoya-Castillo, A. Kelly, and T. E. Markland, "Efficient construction of generalized master equation memory kernels for multi-state systems from nonadiabatic quantum-classical dynamics," J. Chem. Phys. **150**, 244109 (2019).
[44]E. Mulvihill, A. Schubert, X. Sun, B. D. Dunietz, and E. Geva, "A modified approach for simulating electronically nonadiabatic dynamics via the generalized quantum master equation," J. Chem. Phys. **150**, 034101 (2019).
[45]E. Mulvihill, X. Gao, Y. Liu, A. Schubert, B. D. Dunietz, and E. Geva, "Combining the mapping Hamiltonian linearized semiclassical approach with the generalized quantum master equation to simulate electronically nonadiabatic molecular dynamics," J. Chem. Phys. **151**, 074103 (2019).
[46]E. Mulvihill, K. M. Lenn, X. Gao, A. Schubert, B. D. Dunietz, and E. Geva, "Simulating energy transfer dynamics in the Fenna-Matthews-Olson complex via the modified generalized quantum master equation," J. Chem. Phys. **154**, 204109 (2021).
[47]E. Mulvihill and E. Geva, "A road map to various pathways for calculating the memory kernel of the generalized quantum master equation," J. Phys. Chem. B **125**, 9834–9852 (2021).
[48]D. Brian and X. Sun, "Generalized quantum master equation: A tutorial review and recent advances," Chin. J. Chem. Phys. **34**, 497–524 (2022).
[49]G. Amati, M. A. C. Saller, A. Kelly, and J. O. Richardson, "Quasiclassical approaches to the generalized quantum master equation," J. Chem. Phys. **157**, 234103 (2022).
[50]Y. Wang, E. Mulvihill, Z. Hu, N. Lyu, S. Shivpuje, Y. Liu, M. B. Soley, E. Geva, V. S. Batista, and S. Kais, "Simulating open quantum system dynamics on NISQ computers with generalized quantum master equations," J. Chem. Theory Comput. **19**, 4851–4862 (2023).
[51]Y. Liu, E. Mulvihill, and E. Geva, "Combining the generalized quantum master equation approach with quasiclassical mapping Hamiltonian methods to simulate the dynamics of electronic coherences," J. Chem. Phys. **161**, 164101 (2024).
[52]N. Makri, "Discrete generalized quantum master equations," J. Chem. Theory Comput. **21**, 5037–5048 (2025).
[53]R. Peng, L. P. Lindoy, and J. Lee, "On the discretization error of the discrete generalized quantum master equation," J. Chem. Phys. **163**, 134101 (2025).
[54]Y. Tanimura and R. Kubo, "Time evolution of a quantum system in contact with nearly Gaussian-Markoffian noise bath," J. Phys. Soc. Jpn. **58**, 101–114 (1989).
[55]Y. Tanimura, "Stochastic Liouville, Langevin, Fokker–Planck, and master equation approaches to quantum dissipative systems," J. Phys. Soc. Jpn. **75**, 082001 (2006).
[56]Y. Tanimura, "Numerically 'exact' approach to open quantum dynamics: The hierarchical equations of motion (HEOM)," J. Chem. Phys. **153**, 020901 (2020).
[57]Q. Shi, L. Chen, G. Nan, R. Xu, and Y. Yan, "Electron transfer dynamics: Zusman equation versus exact theory," J. Chem. Phys. **130**, 164518 (2009).
[58]S. Mukamel, *Principles of Nonlinear Optical Spectroscopy* (Oxford University Press, Oxford, 1995).
[59]E. Mulvihill and E. Geva, "Simulating the dynamics of electronic observables via reduced-dimensionality generalized quantum master equations," J. Chem. Phys. **156**, 044119 (2022).

[60]J. Cerrillo and J. Cao, "Non-Markovian dynamical maps: Numerical processing of open Quantum trajectories," Phys. Rev. Lett. **112**, 110401 (2014).
[61]A. Nitzan, *Chemical Dynamics in Condensed Phases* (Oxford University Press, New York, 2006).
[62]G. Lindblad, "On the generators of quantum dynamical semigroups," Commun. Math. Phys. **48**, 119 (1976).
[63]B. B. Laird, J. Budimir, and J. L. Skinner, "Quantum-mechanical derivation of the Bloch equations: Beyond the weak coupling limit," J. Chem. Phys. **94**, 4391 (1991).
[64]S. Jang, J. Cao, and R. J. Silbey, "Fourth order quantum master equation and its Markovian bath limit," J. Chem. Phys. **116**, 2705 (2002).
[65]E. Crowder, L. Lampert, G. Manchanda, B. Shoffeitt, S. Gadamsetty, Y. Pei, S. Chaudhary, and D. Davidović, "Invalidation of the Bloch-Redfield equation in the sub-Ohmic regime via a practical time-convolutionless fourth-order master equation," Phys. Rev. A **109**, 052205 (2024).
[66]Z. Xia, J. Garcia-Nila, and D. A. Lidar, "Markovian and non-Markovian master equations versus an exactly solvable model of a qubit in a cavity," Phys. Rev. Appl. **22**, 014028 (2024).
[67]T. Becker, A. Schnell, and J. Thingna, "Canonically consistent quantum master equation," Phys. Rev. Lett. **129**, 200403 (2022).
[68]M. Xu, L. Song, K. Song, and Q. Shi, "Convergence of high order perturbative expansions in open system quantum dynamics," J. Chem. Phys. **146**, 064102 (2017).
[69]C. Wang, J. Ren, and J. Cao, "Nonequilibrium energy transfer at nanoscale: A unified theory from weak to strong coupling," Sci. Rep. **5**, 11787 (2015).
[70]C. Hsieh, J. Liu, C. Duan, and J. Cao, "A nonequilibriium variational polaron theory to study quantum heat transport," J. Phys. Chem. C **123**, 17196–17204 (2019).
[71]X. Dan, P. Khazaei, B. C. Allen, N. Lyu, C. Wilson, E. Mulvihill, Y. Wang, S. Shivpuje, S. Kais, V. S. Batista, and E. Geva, "QFlux: An open-source toolkit for quantum dynamics simulations on quantum computers. Part VI—The generalized quantum master equation," chemRxiv:10.26434/chemrxiv.10001770/v1 (2026).
[72]N. Lyu, E. Mulvihill, M. B. Soley, E. Geva, and V. S. Batista, "Tensor-train thermo-field memory kernels for generalized master equations," J. Chem. Theory Comput. **19**, 1111–1129 (2023).
[73]Q. Shi, Y. Xu, Y. Yan, and M. Xu, "Efficient propagation of the hierarchical equations of motion using the matrix product state method," J. Chem. Phys. **148**, 174102 (2018).
[74]X. Dan and Q. Shi, "Theoretical study of nonadiabatic hydrogen atom scattering dynamics on metal surfaces using the hierarchical equations of motion method," J. Chem. Phys. **159**, 044101 (2023).
[75]N. Lambert, T. Raheja, S. Cross, P. Menczel, S. Ahmed, A. Pitchford, D. Burgarth, and F. Nori, "QuTiP-BoFiN: A bosonic and fermionic numerical hierarchical-equations-of-motion library with applications in light-harvesting, quantum control, and single-molecule electronics," Phys. Rev. Res. **5**, 013181 (2023).
[76]X. Dan, E. Geva, and V. S. Batista, "Simulating non-Markovian quantum dynamics on NISQ computers using the hierarchical equations of motion," J. Chem. Theory Comput. **21**, 1530–1546 (2025).
[77]X. Dan, Z. Long, T. Qiu, J. P. Menzel, Q. Shi, and V. S. Batista, "Nonadiabatic H-atom scattering channels on Ge(111) elucidated by the hierarchical equations of motion," J. Chem. Phys. **164**, 024115 (2026).
[78]H. Breuer and F. Petruccione, *The Theory of Open Quantum Systems* (Oxford Press, Oxford, 2002).
[79]A. Ishizaki and G. R. Fleming, "Theoretical examination of quantum coherence in a photosynthetic system at physiological temperature," Proc. Natl. Acad. Sci. U. S. A. **106**, 17255–17260 (2009).
[80]U. Weiss, *Quantum Dissipative Systems*, 4th ed. (World Scientific, New Jersey, 2012).
[81]A. Kato and Y. Tanimura, "Quantum heat current under non-perturbative and non-Markovian conditions: Applications to heat machines," J. Chem. Phys. **145**, 224105 (2016).
[82]W. Guan, P. Bao, J. Peng, Z. Lan, and Q. Shi, "mpsqd: A matrix product state based Python package to simulate closed and open system quantum dynamics," J. Chem. Phys. **161**, 122501 (2024).